



P-ISSN: 2349-8528

E-ISSN: 2321-4902

www.chemijournal.com

IJCS 2022; 10(5): 98-105

© 2022 IJCS

Received: 15-06-2022

Accepted: 19-07-2022

PK Vishwakarma

Coordination, Bioinorganic and Computational Chemistry Laboratory, Department of P.G. Studies and Research in Chemistry and Pharmacy, Rani Durgavati Vishwavidyalaya, Jabalpur, Madhya Pradesh, India

RC Maurya

Coordination, Bioinorganic and Computational Chemistry Laboratory, Department of P.G. Studies and Research in Chemistry and Pharmacy, Rani Durgavati Vishwavidyalaya, Jabalpur, Madhya Pradesh, India

Design, synthesis and spectral, thermal studies and insilco biological study of dioxidovanadium (V) complex

PK Vishwakarma and RC Maurya

Abstract

In the manuscript, we report the synthesis, spectral and thermal investigation of dioxidovanadium (V) complex. The complex was obtained by the treatment of $[\text{VO}(\text{acac})_2]$ with ONS donor Schiff base in 1:1 mole ratio in ethanol yields of $[\text{VO}_2(\text{L})(\text{H}_2\text{O})] \cdot 1/2\text{H}_2\text{O}$ **1** [HL= dehydroaceticacid-N-4-methyl-3-thiosemicarbazone]. The compound was characterized by physicochemical analyses like magnetic measurements, infrared, electronic, NMR spectral, and thermal studies. A thermogravimetric (TG) curve was used to arrive at insights into the thermal stability of one of the synthesized complexes. The resulting pyrolysis was further manipulated to evaluate the related thermodynamic and kinetic parameters. Based on the thermal analysis order of decomposition (n), activation energy (E_a), entropy (ΔS), free energy (ΔG) and enthalpy changes (ΔH) for each of the three stages of the thermal degradation/pyrolysis have also been evaluated. Moreover, Insilco in-vitro biological activities of studied ligand and dioxidovanadium (V) complex were done with <https://www.molinspiration.com> a web tool.

Keywords: Dioxidovanadium (V) complex, thermal, spectroscopy, and insilco biological activity

Introduction

The continuous interest in the coordination chemistry of vanadium is based on the broad area of catalytic and biological properties in relevant systems (da Silva *et al.* 2013) [11]. The investigation of numerous medicinal properties of vanadium compounds especially in two different oxidation stages +4 and +5 are generally regarded to have insulin-enhancing properties and anti-diabetic effects both *in vivo* and *in vitro* (Thompson *et al.* 2006) [27]. Simple inorganic vanadium salts with different chemical valencies (V(IV) and V(V)) have beneficial biological properties, similar to sodium orthovanadate and vanadyl sulfate. However, these salts caused side effects, when orally administrated to diabetic rats (Shrivastava *et al.* 2005) [26]. The vanadium complexes have grown enormously over the previous few decades due to the role of vanadium in several biological processes, such as haloperoxidation (Macedo-Ribeiro *et al.* 1999) [17], phosphorylation (Corman *et al.* 1995) [9] and glycogen metabolism (Crans *et al.* 1989; Nour-Elden *et al.* 1985) [10, 23]. More recently, vanadium (IV) coordination compounds have been shown to catalyze selective oxidation of alkenes by molecular oxygen (Chatterjee *et al.* 2004) [7]. Vanadium (V) in particular, in stereo-chemically flexible coordination geometries ranging from tetrahedral and octahedral to trigonal pyramidal and pentagonal bipyramidal, is thermodynamically plausible (Djordjevic *et al.* 1998) [13].

Thermal analysis techniques were extensively used in studying the thermal behavior of metal complexes (Soliman *et al.* 2001) [25]. The data provided information concerning the thermal stability and thermal decomposition of these compounds in the solid state. Thermogravimetry is a process in which a substance is decomposed in the presence of heat, which causes the bonds of the molecules to be broken (Albano *et al.* 2000; Carrasco *et al.* 1993) [1, 6]. Kinetic studies of thermal decomposition reactions may become useful in calculating the parameters like the order of reaction (n), activation energy (E_a), entropy change (ΔS), enthalpy change (ΔH), free energy change (ΔG), and pre-exponential factor (z). The number of Schiff bases and their metal complexes provided a rich platform for various interesting biological effects like antibacterial, antifungal, anticancer, anti-inflammatory, antimalarial, and various other effects. Therefore, considering the above facts and continuing our interest in this field, the present work reports a study on the synthesis, spectral characterization, thermal investigation, and Insilco biological activities of dioxidovanadium (V) complex.

Corresponding Author:**PK Vishwakarma**

Coordination, Bioinorganic and Computational Chemistry Laboratory, Department of P. G. Studies and Research in Chemistry and Pharmacy, Rani Durgavati Vishwavidyalaya, Jabalpur, Madhya Pradesh, India

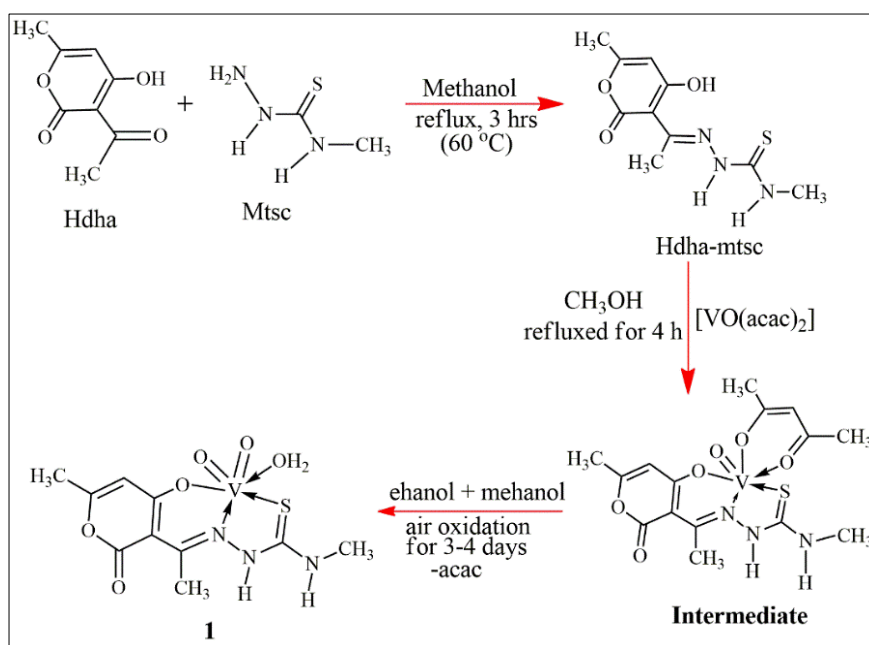
Experimental

Materials and methods: Dehydroacetic acid and methanol (E. Merck, Germany), 4-methyl-3-thiosemicarbazide (Alfa Aesar Division, Johnson Matthey chemicals Pvt. Ltd, USA), were used as received. $[\text{VO}(\text{acac})_2]$ was a prepared method described by (Patel *et al.* 1981) [24]. All chemicals used were of analytical reagent (A. R.) grade. The infrared spectral analysis ($400\text{--}4000\text{ cm}^{-1}$) was recorded on a Bruker $\alpha\text{-T}$ FTIR spectrophotometer, with KBr pellets. Electronic spectral analysis was recorded on a CARY-5000, UV-VIS-NIR spectrophotometer in quartz cells. The magnetic measurement was carried out using mercury (II) tetrathiocyanatocobaltate (II) as a calibrant on Sherwood Scientific magnetic susceptibility balance (UK). Thermogravimetric analysis was done by heating the sample at a rate of $25\text{ }^\circ\text{C min}^{-1}$ up to $1000\text{ }^\circ\text{C}$ on a thermal analyzer at Sophisticated Analytical Instrument Facility, IIT, Mumbai. Elemental analysis was performed on an Elemental Vario ELIII Carlo Erba 1108 analyzer from SAIF, CDRI, Lucknow.

Synthesis of Schiff base: Ligand (HL) was prepared by following the method (Scheme 1). Yield: 0.3978g, (78%). Melting point: $216\text{ }^\circ\text{C}$. Anal. Calc. for $\text{C}_9\text{H}_{11}\text{N}_3\text{O}_3\text{S}$ (MW: 255): C, 47.05; H, 5.13; N, 16.46, Found: C, 46.14; H, 4.96; N, 18.40%. Solubility: Methanol, Acetonitrile, DMF, and

DMSO. IR (KBr, $4000\text{--}500\text{ cm}^{-1}$): $\nu(\text{C}=\text{O})$ 1678s, $\nu(\text{C}=\text{N})$ 1648s, $\nu(\text{C}-\text{O})$ 1342, $\nu(\text{C}=\text{S})$ 1168. IUPAC Name: 4-hydroxy-6-methyl-2-oxo-2H-pyran-3-yl-ethylidene-N-methylcarbamohydrazone-thioic acid.

Synthesis of $[\text{VO}_2(\text{L})(\text{H}_2\text{O})]\cdot\frac{1}{2}\text{H}_2\text{O}$ 1: A hot methanolic solution of $[\text{VO}(\text{acac})_2]$ (0.001M, 0.266 g) in 20 mL, was added to the equimolar amount of the respective Schiff base ligand, HL (0.255 g) dissolved in 20 mL of methanol were mixed. The resulting solution was refluxed for 4 h at $60\text{ }^\circ\text{C}$. It was cooled and filtered. The filtrate was collected and the precipitate was dissolved in ethanol-methanol (1:10) and again filtered. The filtrate thus obtained is again added to the above filtrate, which is then kept for air oxidation at room temperature for 3-4 days with occasional shaking. The resulting compound is collected and recrystallized from methanol. $[\text{VO}_2(\text{L})(\text{H}_2\text{O})]\cdot\frac{1}{2}\text{H}_2\text{O}$ 1 Yield: 0.2484g, (68%). Melting point: $253\text{ }^\circ\text{C}$. Anal. Calc. for: $\text{C}_{10}\text{H}_{13}\text{N}_3\text{O}_6\text{SV}$, (MW: 365.25): C, 33.91; H, 3.70; N, 11.86; S, 9.05. Found: C, 33.81; H, 3.63; N, 11.82; S, 9.12. Solubility: Methanol, Acetonitrile, DMF, and DMSO. IR (KBr, $4000\text{--}600\text{ cm}^{-1}$): $\nu(\text{C}=\text{O})$ 1715, $\nu(\text{C}=\text{N})$ 1580, $\nu(\text{C}-\text{O})$ 1324, $\nu(\text{C}=\text{S})$ 1140, $\nu_s(\text{VO}_2)$ 960, $\nu_{as}(\text{VO}_2)$ 880 cm^{-1} . UV-Vis (DMSO) λ_{max} nm: 265, 319.



Scheme 1: Synthetic route of dioxidovanadium (V) complexes

Thermodynamic Studies

In the present investigation, we work with two thermal methods the non-isothermal mode for TGA techniques from (i) Coats-Red method and (ii) the Broido method. The order of reaction activation energy (E_a), enthalpy (ΔH), entropy (ΔS), and free energy changes (ΔG) were also calculated at a particular step.

The Coats-Red fern equations (Coats *et al.* 1964) [8] are in the following form:

$$\ln \left[\frac{1-(1-\alpha)^{\frac{1}{n}}}{(1-\alpha)T^2} \right] = \frac{M}{T+B} \text{ for } n \neq 1 \quad \dots \text{ (i)}$$

$$\ln \left[\frac{-\ln(1-\alpha)}{T^2} \right] = \frac{M}{T+B} \text{ for } n = 1 \quad \dots \text{ (ii)}$$

Where α represents the fraction of sample decomposed at time t , defined by

$$\alpha = \frac{(W_0 - W_t)}{(W_0 - W_\infty)} \quad \dots \text{ (iii)}$$

W_0 , W_t , and W_∞ are the weight of the sample before the degradation, at temperature $t\text{ }^\circ\text{C}$, and after total conversion respectively. T is the derivative peak temperature

$$M = -\frac{E_a}{R} \text{ \& } B = \frac{\ln AR}{\phi E_a}$$

E_a , R , A , and ϕ are the heat of activation, the universal gas constant, the pre-exponential factor, and the heating rate respectively. The correlation coefficient 'r' was computed

using the least square method for different values of n ($n=0.33, 0.5, 0.66, \text{ and } 1$), by plotting the LHS of equation (i) or (ii) versus $1/TK$. The n values which gave the best fit ($n \approx 1$) were chosen as the order parameter for the decomposition stage of interest. From the intercept and linear slope of the such stage, the Z and E_a values were determined. ΔS was also computed using the relationship:-

$$\Delta S = \left[\left(\ln \frac{Zh}{KT} \right) - 1 \right] \quad \dots \text{(iv)}$$

$$\Delta H = E_a - RT \quad \dots \text{(v)}$$

$$\Delta G = \Delta H - T\Delta S \quad \dots \text{(vi)}$$

Where, K_B is the Boltzmann's constant, h is Planck's constant and T_m is the DTG peak temperature. ΔH and ΔG are calculated using equations (v) and (vi).

Broido Method: Broido has developed a model (Broido *et al.* 1969) [4] and put forward a simple and sensitive graphical method for the treatment of TGA data. According to this method, the weight at any time t (W_t) is related to the fraction of initial molecular weight as shown below.

$$Y = \frac{N}{N_0} = \frac{W_t - W_a}{W_0 - W_a} \quad \dots \text{(vii)}$$

Where

W_0 is the initial weight of the materials and

W_a is the weight of residue at the end of decomposition:

For isolated pyrolysis:

$$\frac{dy}{dt} = -Ky^n \quad \dots \text{(viii)}$$

$$\text{If, } K = Ae^{-E/RT} \quad \dots \text{(ix)}$$

and if T is a linear fraction of time t , therefore:

$$T = T_0 + \beta t \quad \dots \text{(x)}$$

$$\frac{dy}{dn} = -\frac{A}{\beta} e^{E/RT} . dt \quad \dots \text{(xi)}$$

Where

$\beta = dT/t$, the heating rate Eq. (xi) is integrated as:

$$\int_Y^1 \frac{dy}{dn} = \frac{A}{\beta} \int_{T_0}^T e^{-E/RT} . dt \quad \dots \text{(xii)}$$

For the first order kinetics ($n=1$) in which complex degrades usually:

$$\int_Y^1 \frac{dy}{y} = - \ln y = \ln \left(\frac{1}{y} \right) \quad \dots \text{(xiii)}$$

On integrating and taking the log of both sides of Eq. (xiii), the following equation is obtained.

$$\ln \left[\ln \left(\frac{1}{y} \right) \right] = \left(\frac{E}{RT_{m+1}} \right) \ln T + \text{Constant} \quad \dots \text{(xiv)}$$

Thus, a plot of $\ln \left[\ln \left(\frac{1}{y} \right) \right]$ v/s $1/T$ yields a straight line, whose slope is directly related to E_a :

$$-E_a = \text{Slope} \times 2.303 \times R \quad \dots \text{(xiv)}$$

Where E_a is the activation energy and R is the gas constant. The application of this method is used to determine the kinetic parameter for the complexes.

$$\ln \left[\ln \left(\frac{1}{Y} \right) \right] = \left(\frac{-E_a}{R} \right) \frac{1}{T} + \left[\frac{RZ}{E_a \phi T_m^2} \right] \quad \dots \text{(xv)}$$

Where

$Y = \frac{W_f - W_{\infty}}{W_0 - W_{\infty}}$ and Z can be calculated from the relation

$$Z = \left(\frac{E_a \phi}{RT_m^2} \right) \frac{1}{T} + \left[\frac{RZ}{E_a \phi T_m^2} \right]$$

ΔH and ΔG are calculated using equations (v) and (vi)

Results and discussion

Infrared spectral studies: The infrared spectrum of Schiff base show a weak band at 3448 cm^{-1} for $\nu(\text{O-H})$, a strong band at 1678 cm^{-1} for $\nu(\text{C=O})$ (lactone), and another strong band at 1648 cm^{-1} due to $\nu(\text{C=N})$ (azomethine). The presence of both $\nu(\text{N-H})$ (hydrazide) and $\nu(\text{N-H})$ of (thioamide) peaks are found to be merged at 3268 cm^{-1} . The presence of a medium band at 1168 cm^{-1} in the ligand is most probably due to $\nu(\text{C=S})$ of the thiosemicarbazone moiety (Banwell *et al.* 1997) [2]. These observations suggest that the ligand under the present investigation exists in thione form. In the coordination of enolic oxygen after deprotonation, the $\nu(\text{OH})$ at 3448 cm^{-1} should be disappeared in the spectra of the complex. But due to the presence of $\nu(\text{OH})$ on account of coordinated water (vide infra), it is difficult to say the coordination of enolic oxygen after deprotonation with certainty. However, such coordination is supported by the appearance of $\nu(\text{C-O})$ (enolic) at 1315 cm^{-1} compared to $\nu(\text{C-O})$ (enolic) at 1342 cm^{-1} in the ligand. The $\nu(\text{C=S})$ mode of the thione group observed at 1249 cm^{-1} in the ligand is shifted to lower wave numbers (Maurya *et al.* 1995) [20] and appears at 1168 cm^{-1} in the complex. This suggests the bonding of the thione sulfur to vanadium in the complex. A sharp and strong band at 1648 cm^{-1} is due to $\nu(\text{C=N})$ in the ligand after the complexation this band is observed at 1573 cm^{-1} suggesting the coordination of the azomethine nitrogen to vanadium. The overall infrared spectral studies conclude that the thiosemicarbazones used in the present study behave as monobasic tridentate ONS-donor ligands. The metal chelates also show a medium/broadband at 3427 cm^{-1} due to $\nu(\text{OH})$ mode because of the presence of lattice/coordinated water in them. Complex 1 display a sharp two sharp medium bands at $850\text{-}902 \text{ cm}^{-1}$ corresponding to $\nu_{as}(\text{O=V=O})$ and $\nu_s(\text{O=V=O})$ modes (Maurya *et al.* 2002) [19] respectively.

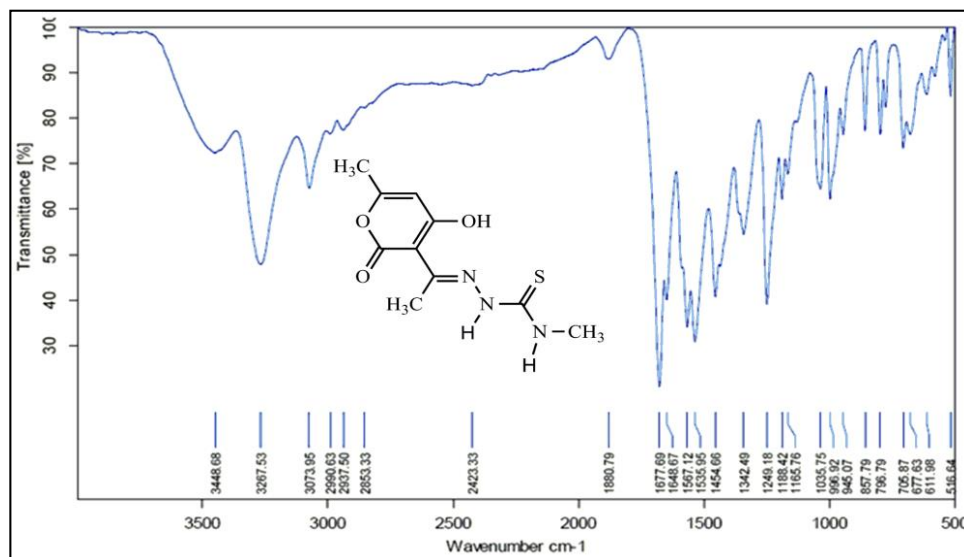


Fig 1: Experimental FTIR Spectrum of synthesized ligand HL.

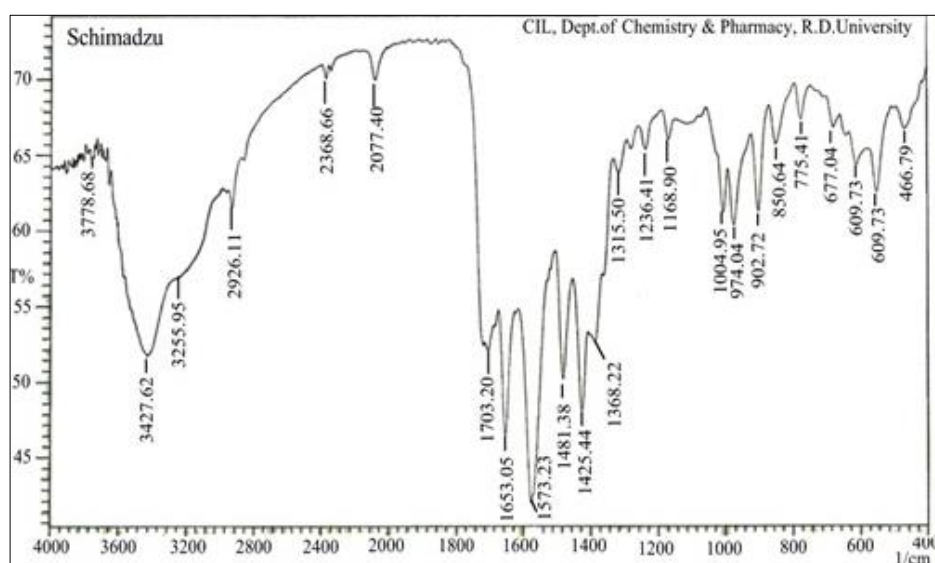


Fig 2: Experimental FTIR Spectrum of complex $[\text{VO}_2(\text{L})(\text{H}_2\text{O})] \cdot \frac{1}{2}\text{H}_2\text{O}$

The electronic spectral analysis: The electronic spectra of the ligand HL and their complex 1 shown in (Figure 3) were recorded in 10^{-3} M DMSO solutions. The ligand HL displayed two peaks at 282 and 318 nm the peaks are assigned intra-ligand transitions. While complex 1 displayed three peaks at

284, 344, and 415 nm. The first two peaks at 284 and 344 nm assign intra-ligand transitions in the ultraviolet region and the 3rd spectral peak at ~ 415 nm is due to ligand \rightarrow metal charge transfer (LMCT) transition.

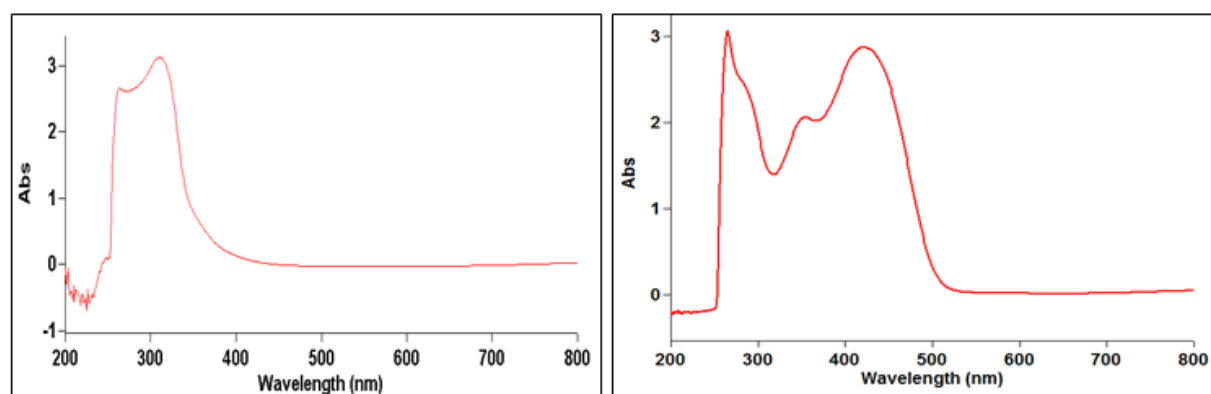


Fig 3: Electronic spectrum of ligand HL (left) and complex 1 (right).

Conductance Magnetic measurements: The molar conductance values of the synthesized complexes in 10^{-3} M DMF solution is in the range of $14.6\text{-}16.9 \text{ ohm}^{-1}\text{cm}^2 \text{ mol}^{-1}$.

These results are indicative of the non-electrolytic nature of these complexes. The non-zero conductance values are most probably due to the strong donor capacity of DMF, which

may lead to the displacement of anionic ligand and a change of electrolyte type (Maurya *et al.* 2016) [22]. All the oxidovanadium (IV) complex is paramagnetic and diamagnetic as expected for dioxidovanadium (V) (Maurya *et al.* 2015) [21].

¹HMR spectral studies: The proton ¹H-NMR spectrum of a diamagnetic compound **2** was recorded in DMSO-d₆, using TMS as a reference and presented in Figure 4. This compound displays a singlet peak due to heteroaromatic proton (dha

moiety) signal at δ 5.98 ppm (a), and at δ 2.12 (b) and δ 2.16 ppm (c) due to –NH proton of hydrazide moiety. The proton signals at δ 2.503-3.45 ppm (d & e) and 1.236 ppm (f) are most probably due to methyl proton groups present in this compound. The proton signal is at 2.5. ppm is most probably due to the solvent (DMSO-d₆) taken. The absence of an enolic proton signal at ~ 12 ppm in the complex indicates the coordination of enolic oxygen to the metal ion after deprotonation. The indexing of various proton groups is given in scheme 3.

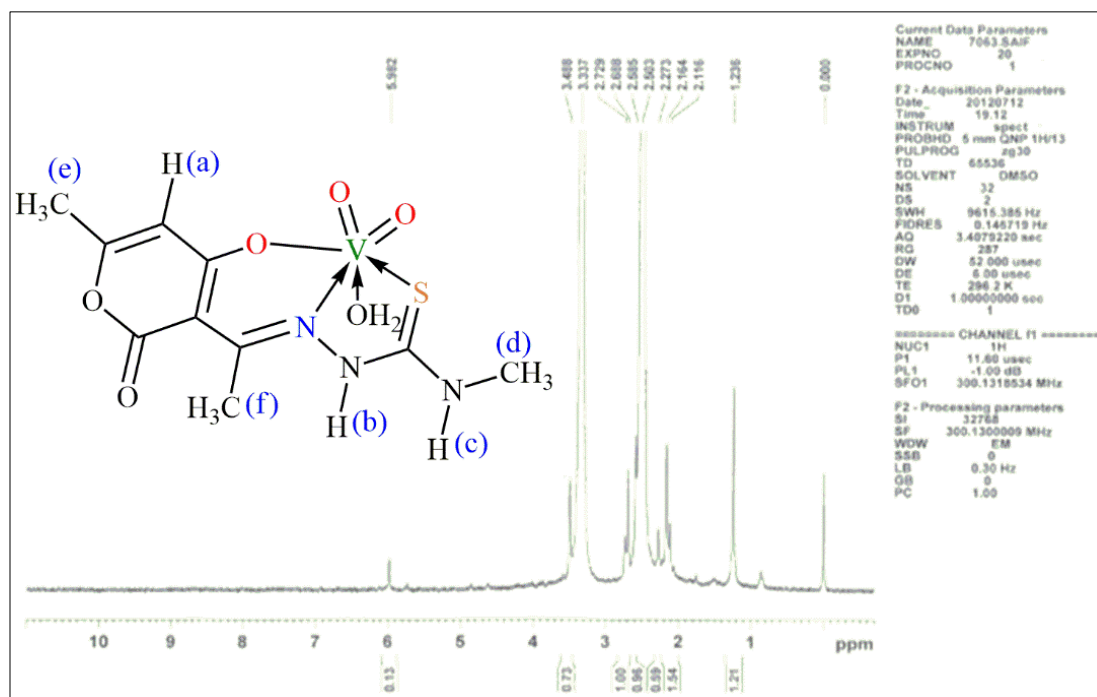


Fig 4: ¹H-NMR of **1** with the indexing of various proton groups.

Thermogravimetric studies: Thermogravimetric study of compound **1** in (Figure 5) was subjected to thermogravimetric analysis in the temperature range 25-1000 °C at the heating rate of 10 °C/min. Compound **1** shows a first weight loss of observed 2.239 % at 88°C calculated to the elimination of half mole lattice water and a second weight loss of 3.99% at 165 °C (calcd. weight loss of one mole H₂O, 4.13%) corresponding to the elimination of one molecule of

coordinated water. This compound shows further weight losses beyond 253, 502 and upto 980 °C the weight losses of 15.41, 34.73 and 19.99% respectively, However, the final weight loss of 75.6% observed at 980 °C corresponds to the elimination of one (HL) ligand group (calcd. weight loss, 70.128%). The final residue (obs. = 24.1%) roughly corresponds to V₂O₅ (calcd. = 29.872%).

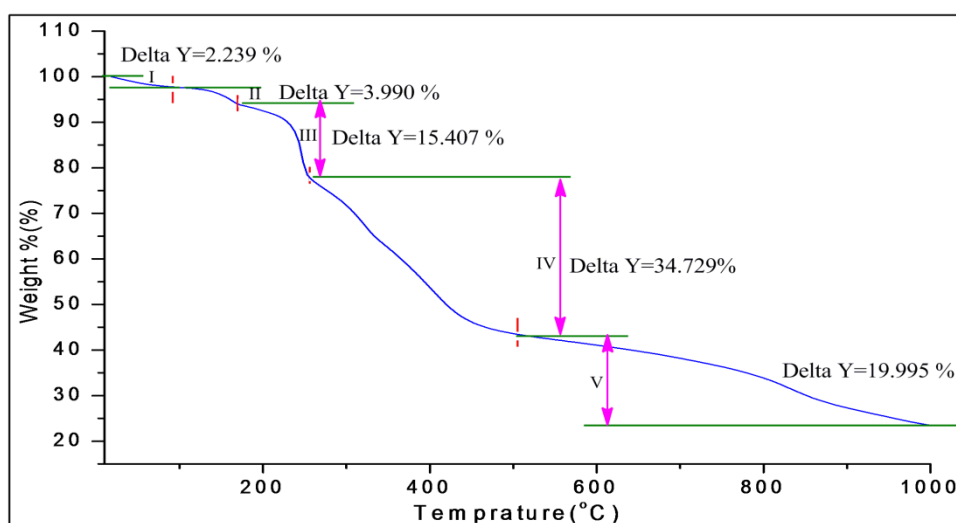


Fig 5: TGA curve of synthesized complex [VO₂(L)(H₂O)].¹/₂H₂O **1**

Thermodynamic Studies Based on TGA: The thermogram of the representative compound provided generous proof in all the methods reflecting the order of the decomposition of the order (n) of unity. The kinetic and thermodynamic parameters of the thermal degradation of the complexes namely, activation energy (E_a), enthalpy (ΔH), entropy (ΔS), and free energy changes (ΔG) were also calculated against the methods described in the experimental section. The relevant parameters of each involved method at each step of decomposition were evaluated and are given in Table 1. The respective graphical presentations have also been given in Figures 6 and 8. The following remarks are pointed out:

- 1) The low negative values of ΔS show that the activated state is more ordered and stable than the reactants (Forst *et al.* 1961) [15].
- 2) In the subsequent decomposition stages of the given complex, values of ΔG increase markedly, although no regular trend is observed in the values of either E_a or ΔH .

It is because ΔS increases from one step to another, an override in the values of ΔH is noticeable. Increasing values of ΔG for the subsequent steps of a given complex reflects that the rate of mass loss will be lower than that of the precedent species (Malavalli *et al.* 1999) [18]. The structural rigidity of the remaining compound gets increased after the expulsion of one or more species, as compared with the precedent complex.

- 3) From the values of ΔG , we may confirm the coordination core where there attains an increase in its value.
- 4) It is known that the order has no intrinsic meaning, but is rather a mathematical smoothing parameter (Brown *et al.* 1980) [5]. In the present case, the reaction order of all the decomposition stages of all the methods is found to be nearly equal to one. The plots are linear with a regression coefficient, r , ranging between 0.970 and 0.999. This result indicates that all three-step decomposition of complex follows the first-order kinetics.

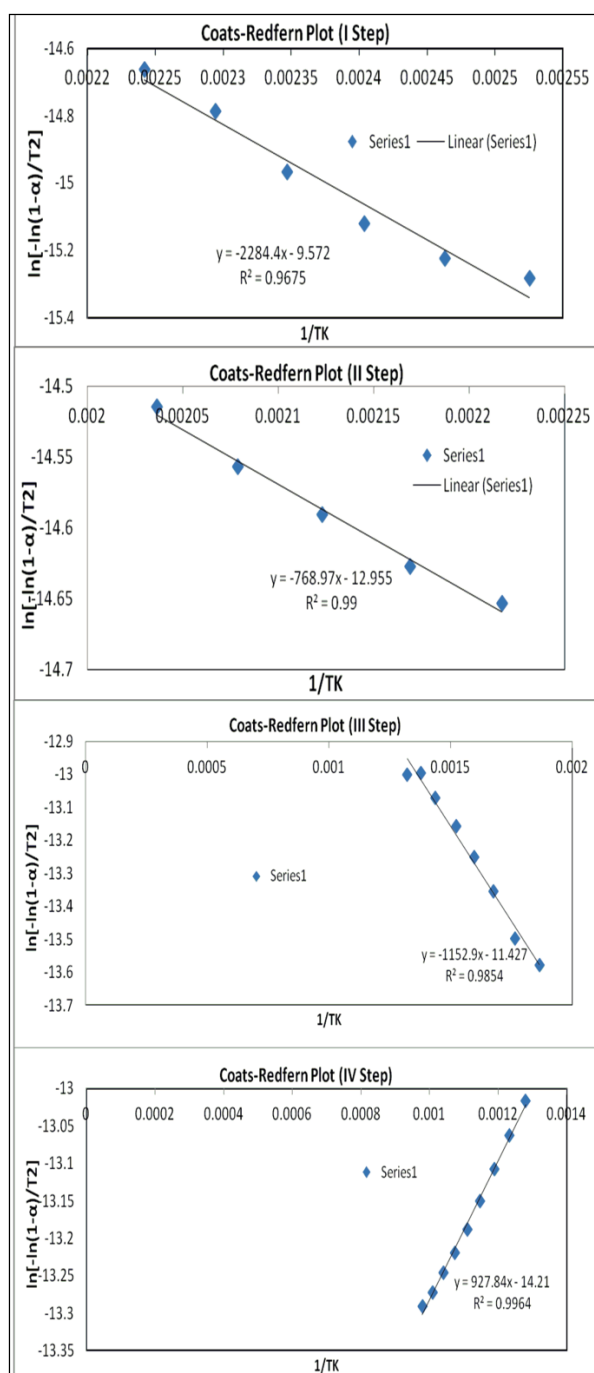


Fig 6: Coats-Redfern plot of complex $[\text{VO}_2(\text{L})(\text{H}_2\text{O})] \cdot \frac{1}{2}\text{H}_2\text{O} \mathbf{1}$

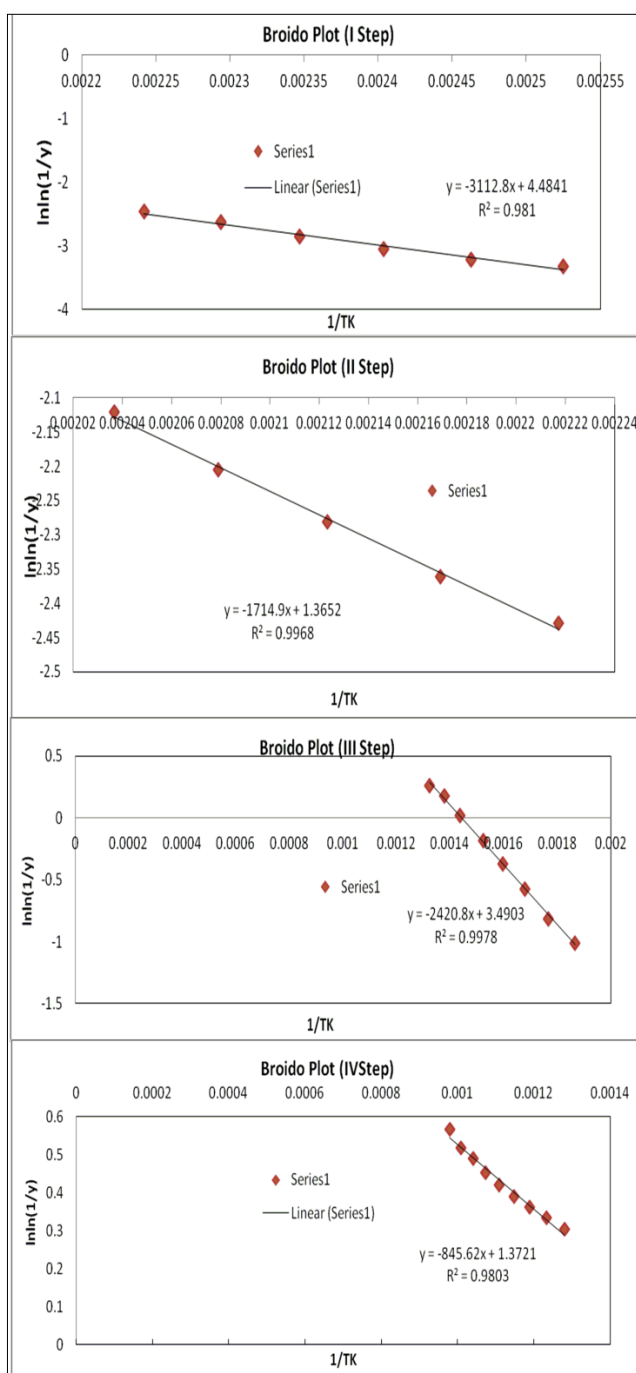


Fig 7: Brando plot of complex $[\text{VO}_2(\text{L})(\text{H}_2\text{O})] \cdot \frac{1}{2}\text{H}_2\text{O} \mathbf{1}$

Bioactivity score Druglikeness properties: The very applicable interaction of drugs with many biological targets *viz.*, enzymes, ion channels, receptors, etc. in living beings define the pharmacological action of drugs. The bioactivity scores are based on numerous parameters that are (i) G-protein coupled receptor ligand (GPCRL), (ii) ion channel modulation (ICM), (iii) nuclear receptor ligand (NRL), (iii) kinase inhibition (KI), (iv) protease inhibition (PI), (v) enzyme inhibition (EI) and the bioavailability of the studied compounds was predicted by subjecting them to calculations through web-server, www.molinspiration.com and these results are presented in Table 2. It has been suggested that compounds with bioactivity scores >0.0 are highly bioactive whereas scores between -5.0 to 0 have moderate activity and <-5.0, then they are inactive. The present studied compounds have values between -1.91 to 0.01, so they are expected to have moderate activity (Dhanaraj *et al.* 2016) [12].

Lipinski's rule of five (RO5) is a benchmark for drug design and their development, it also assists in the description of molecular properties of drug candidates which provided insight into numerous pharmacokinetic parameters *viz.*, absorption, distribution, metabolism, and excretion (ADME) for predicting the success of an orally introduced drugs journey through the body towards the site of action. The rule

predicts the oral activity of a drug candidate in connection with a certain molecular parameter (i) logP (partition coefficient), (ii) molecular weight, (iii) number of hydrogen bond acceptors, (iv) hydrogen bond donors, and (v) polar surface area. According to RO5, an orally active drug candidate should have logP ≤-5, number of hydrogen bond acceptors (≤10), number of hydrogen bond donors (≤5), and molecular weight (≤500) (Lipinski *et al.* 2001) [16]. Normally, an orally active drug should not display any violation according to the rules. Herein, the values of milLogP, TPSA, molecular weight, and other parameters for the studied compound are calculated and charted in Table 3. It can be observed that ligand HL and complex 1 are having milLogP values is 2.59 and -5.16, which is within the tolerable limit of a drug candidate to infiltrate through biomembranes and are displaying good bioavailability as per Lipinski's Rule (Ammal *et al.* 2020) [2]. The ligand and its Cu(II) complex do not show any violation of Lipinski's rule. So, the studied compounds can be considered oral therapeutic molecules as per RO5. But the recent developments in drug discovery have increased the chemical space for oral druggable candidates beyond Lipinski's Rule of 5 (bRo5) by considering target interaction and incorporating various natural products rich in activities (Doak *et al.* 2016) [14].

Table 2: Bioactivity score of the HL and its complex dioxovanadium (V)1.

Comp.	Parameters of Bioactivity score					
	GPCR ligand	Ion channel modulator	Kinase inhibitor	Nuclear receptor ligand	Protease inhibitor	Enzyme inhibitor
HL	-1.81	-1.65	-1.91	-1.61	-0.96	-0.59
1	-0.52	-0.57	-0.70	-0.61	-0.12	0.01

Table 3: Druglikeness score of the HL and its complex dioxovanadium (V)1.

Comp.	Lipinski's Parameters						Lipinski's violations
	% Abs.	TPSA (Å) ²	MlogP	nOHNH	nON	nrtb	
HL	79.33	86.86	1.00	3	6	4	0
1	66.1	124.03	-5.47	4	9	1	0

Percentage absorption was calculated by % Absorption = 109-[0.345×Topological Polar Surface Area] Topological polar surface area (defined as a sum of surfaces of polar atoms in a molecule), Logarithm of compound partition coefficient

between n-octanol and water, Hydrogen bond donors (nOHNH), Hydrogen bond acceptors (nON) and Number of rotatable bonds (nrotb).

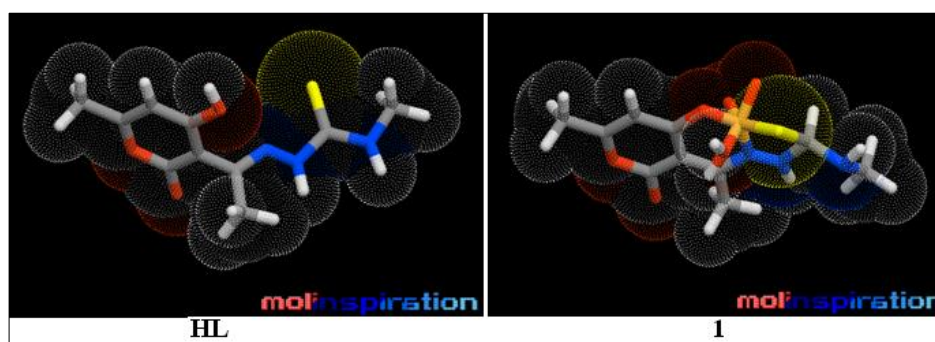


Fig 7: 3D-Molecular structures of ligand (HL) and their complex 1 obtained through Molinspiration galaxy 3D structure generator v2021.01 beta a web-tool.

Conclusion

From the discussions laid so far in favor of the structural elucidation it is suggested that the complex under this investigation may be formulated as, $[\text{VO}_2(\text{L})(\text{H}_2\text{O})] \cdot \frac{1}{2}\text{H}_2\text{O}$,

Where

L = dehydroacetic acid-N-4-methyl-3-thiosemicarbazone. Considering distorted octahedral geometry with a monomeric

Hexa-coordination environment has been proposed. The Thermogravimetric (TG) curve used to arrive at the insights of thermal stability of the complex shows it is thermally stable to a higher temperature range and the final oxide derivative possesses the highest stability among the different pyrolytic fragments intervened in the course of the TG experiment. Insilco biological screening indicates that the studied ligand

and its complex are good drug candidates possessing diverse biological activities.

Acknowledgments

The authors are highly acknowledging our Vice-Chancellor, Professor Kapil Deo Mishra, for their blessing, support, and motivation. We are also thankful to our Head of the department, for encouraging and providing instrumentational facilities at the Department. In addition, analytical facilities provided by the SAIF, Central Drug Research Institute, Lucknow are gratefully acknowledged.

Author contributions

PKV: Synthesis work, data collection, theoretical work, and writing manuscript. RCM: research plan final drafting manuscript. The authors contributed to the article and approved the submitted version.

Disclosure statement

The authors declared that no war of interest with this work.

References

- Albano ACL, Sciamanna R, Aquino T, Martinez JJ. European Congress on Computational Methods in Applied Sciences and Engineering, ECO MAS 2000, Barcelona; c2000, p, 11-14.
- Ammal PR, Prasad AR, Joseph A. Synthesis, characterization, in silico, and *in vitro* biological screening of coordination compounds with 1,2,4-triazine based biocompatible ligands and selected 3d-metal ions. *Heliyon*, 2020. <https://doi.org/10.1016/j.heliyon.2020.e05144>.
- Banwell CN, McCash EM. *Fundamentals of Molecular Spectroscopy*, 4th edition, Tata McGraw Hill Publishing Company Ltd., New Delhi, 1997, 86.
- Broido A. A simple, sensitive graphical method of treating thermogravimetric analysis data. *J. Polym. Sci. A-2 Polym Phys.* 1969;7:1761-1773.
- Brown DB, Walton EG, Dits JA. Thermal reactions of the mixed-valence iron fluorides, Fe₂F₆·nH₂O. *J. Chem. Soc. Dalton Trans.* 1980;662:845-850.
- Carrasco F. The evaluation of kinetic parameters from thermogravimetric data: comparison between established methods and the general analytical equation. *Thermochim. Acta.* 1993;213:115-134.
- Chatterjee D, Mitra A. Synthesis, Characterization and reactivities of Schiff-base complexes of Ruthenium (III). *J. Coord. Chem.* 2004;57:175-182.
- Coats AW, Redfern IP. Kinetic Parameters from Thermogravimetric Data. *Nature.* 1964;20:68-69.
- Cornman CR, Zovinka EP, Meixner MH. Vanadium (IV) Complexes of an Active-Site Peptide of a Protein Tyrosine Phosphatase. *Inorg. Chem.* 1995;34:5099-5100.
- Crans DC, Bunch RL, Theisen LA. Interaction of trace levels of vanadium (IV) and vanadium (V) in biological systems. *J. Am. Chem. Soc.* 1989;111:7597-7607.
- da Silva JAL, da Silva JJRF, Pombeiro AJL. Amavadin, a vanadium natural complex: Its role and applications *Coord. Chem. Rev.* 2012;257:2388-2400.
- Dhanaraj CJ, Johnson J. Studies on some metal complexes of quinoxaline based unsymmetric ligand: synthesis, spectral characterization, *in vitro* biological and molecular modeling studies, *J Photochem. Photobiol. B Biol.* 2016;161:108-121.
- Djordjevic C, Puryear PC, Vuletic N, Allelt CJ, Sheffield SJ. Preparation, spectroscopic properties, and characterization of novel peroxo complexes of vanadium (V) and molybdenum (VI) with nicotinic acid and nicotinic acid N-oxide. *Inorg. Chem.* 1998;27:2926-2932.
- Doak BC, Kihlberg J. How beyond rule of 5 drugs and clinical candidates bind to their targets, *J. Med. Chem.* 2016;59:2312-2327.
- Forst AA, Pearson RG. *Kinetics and Mechanisms*, Wiley, New York, 1961.
- Lipinski CA, Lombardo F, Dominy BW, Feeney PJ. Experimental and computational approaches to estimate solubility and permeability in drug discovery and development settings, *Adv. Drug Deliv. Rev.* 2001;46:3-26.
- Macedo-Ribeiro S, Hemrika W, Renirie R, Wever R, Messerschmidt A. X-ray crystal structures of active site mutants of the vanadium-containing chloroperoxidase from the fungus *Curvularia inaequalis*. *J. Biol. Inorg. Chem.* 1999;4:209-219.
- Maravalli PB, Goudar TR. Thermal and spectral studies of 3-*N*-methyl-morpholino-4-amino-5-mercapto-1,2,4-triazole and 3-*N*-methyl-piperidino-4-amino-5-mercapto-1,2,4-triazole complexes of cobalt(II), nickel(II) and copper(II). *Thermochim. Acta.* 1999;325:35-41.
- Maurya MR, Khurana S, Zhang W, Rehder D. Biomimetic oxo-, dioxo- and oxo-peroxo-hydratonato-vanadium(IV/V) complexes. *J. Chem. Soc. Dalton Trans.* 2002;3015-3023.
- Maurya RC, Mishra DD, Pillai V. Studies on Some Novel Mixed-Ligand Oxovanadium (IV) Complexes Involving Acetylacetonate and Nitrogen or Oxygen Donor Organic Compounds. *Synth. React. Inorg. -Met. Org. Chem.* 1995;25:1127-1141.
- Maurya RC, Sutradhar D, Martin MH, Roy S, Chourasia J, Sharma AK, *et al.* Oxovanadium (IV) complexes of medicinal relevance: Synthesis, characterization, and 3D-molecular modeling and analysis of some oxovanadium (IV) complexes in O, N-donor coordination matrix of sulfa drug Schiff bases derived from a 2-pyrazolin-5-one derivative. *Arab. J. Chem.* 2015;8:78-92.
- Maurya RC, Vishwakarma PK, Mir JM, Rajak DK. Oxidoperoxidomolybdenum (VI) complexes involving 4-formyl-3-methyl-1-phenyl-2-pyrazoline-5-one and some β -diketoenolates. *J. Therm. Anal. Cal.* 2016;124:57-70.
- Nour-Elden AF, Craig MM, Gresser MJ. Interaction of inorganic vanadate with glucose-6-phosphate dehydrogenase. Nonenzymic formation of glucose 6-vanadate. *J. Biol. Chem.* 1985;260:6836-6842.
- Patel KS. Physicochemical studies of metal β -diketonates-VI Magnetic properties of some oxovanadium (IV) β -keto-enolates. *J. Inorg. Nucl. Chem.* 1981;43:667-669.
- Soliman AA. Thermogravimetric and Spectroscopic Studies on Cadmium Complexes with Two Salicylidene Thiophenol Schiff Bases. *J Therm. Anal. Cal* 2001;63:221-231.
- Srivastava AK, Mehdi MZ. Insulino-mimetic and anti-diabetic effects of vanadium compounds. *Diabet. Med.* 2005;22:2-13.
- Thompson KH, Orvig C. Vanadium in diabetes: 100 years from Phase 0 to Phase I. *J Inorg. Biochem.* 2006;100:1925-1935.